Spin Crossover Hot Paper

How to cite: *Angew. Chem. Int. Ed.* **2021**, *60*, 22562–22569
International Edition: doi.org/10.1002/anie.202108792
German Edition: doi.org/10.1002/ange.202108792

A Family of Heterobimetallic Cubes Shows Spin-Crossover Behaviour Near Room Temperature

*Matthias Hardy, Jacopo Tessarolo, Julian J. Holstein, Niklas Struch, Norbert Wagner, Ralf Weisbarth, Marianne Engeser, Johannes Beck, Shinnosuke Horiuchi, Guido H. Clever, and Arne Lützen**

Abstract: *Using 4-(4′-pyridyl)aniline as a simple organic building block in combination with three different aldehyde components together with metal(II) salts gave three different Fe_8Pt_6-cubes and their corresponding Zn_8Pt_6 analogues by employing the subcomponent self-assembly approach. Whereas the use of zinc(II) salts gave rise to diamagnetic cages, iron(II) salts yielded metallosupramolecular cages that show spin-crossover behaviour in solution. The spin-transition temperature $T_{1/2}$ depends on the incorporated aldehyde component, giving a construction kit for the deliberate synthesis of spin-crossover compounds with tailored transition properties. Incorporation of 4-thiazolecarbaldehyde or N-methyl-2-imidazole-carbaldehyde yielded cages that undergo spin-crossover around room temperature whereas the cage obtained using 1H-4-imidazolecarbaldehyde shows a spin-transition at low temperatures. Three new structures were characterized by synchrotron X-ray diffraction and all structures were characterized by mass spectrometry, NMR and UV/Vis spectroscopy.*

Introduction

Metallosupramolecular chemistry[1] is a rapidly developing field which has produced numerous coordination cages with various geometries and architectures.[2] As structural diversity and complexity is increasingly difficult to achieve using monometallic approaches,[3] new strategies have been developed that aim to construct heterobimetallic complexes. This includes the implementation of new designs like the complex-as-a-ligand strategy,[4] leading to more and more studies towards heterobimetallic cages with different shapes and geometries that can be found in the literature.[4,5] Moreover, on the search for new functional materials, heterobimetallic aggregates offer the exciting chance to combine properties of two different metal centres within one discrete structure, potentially expanding its electrochemical,[6] photophysical[7] or magnetic properties.[8]

One prominent magnetic property that has attracted the interest of many researchers is the spin-crossover phenomenon[9] in which a system switches between distinguishable high- and low-spin states upon external stimuli like temperature,[10] light[11] or pressure.[12] Particularly iron(II) based systems have been intensively investigated towards their spin-crossover properties,[10–13] as iron(II) switches between a paramagnetic (high-spin) and a diamagnetic (low-spin) state. This offers the possibility to easily distinguish between both states based on their magnetism and often even their optical properties. Due to this behaviour, spin-crossover systems are interesting materials for several applications that depend on molecular switching.[14] However, low transition temperatures often limit the applicability of spin-crossover systems, and therefore, the search for systems that undergo spin transition near room temperature is a desirable goal. For the development of new spin-crossover materials, supramolecular chemistry has become increasingly important, as supramolecular architectures offer the possibility to mechanically connect several spin-crossover centres in multinuclear complexes like squares and grids,[15] helicates,[16] or tetrahedrons.[10a,17] To date, however, only very few examples of spin-crossover cages

[*] Dr. M. Hardy, Dr. N. Struch, Priv.-Doz. Dr. M. Engeser, Prof. Dr. A. Lützen
Rheinische Friedrich-Wilhelms-Universität Bonn, Kekulé-Institut für Organische Chemie und Biochemie
Gerhard-Domagk-Str. 1, 53121 Bonn (Germany)
E-mail: arne.luetzen@uni-bonn.de

Dr. J. Tessarolo, Dr. J. J. Holstein, Prof. S. Horiuchi, Prof. Dr. G. H. Clever
Technische Universität Dortmund
Otto-Hahn-Str. 6, 44227 Dortmund (Germany)

N. Wagner, Dr. R. Weisbarth, Prof. Dr. J. Beck
Rheinische Friedrich-Wilhelms-Universität Bonn, Institut für Anorganische Chemie
Gerhard-Domagk-Str. 1, 53121 Bonn (Germany)

Prof. S. Horiuchi
Division of Chemistry and Materials Science, Graduate School of Engineering, Nagasaki University
Bunkyo-machi, Nagasaki, 852-8521 (Japan)

Dr. M. Hardy
Current address: BASF SE
Speyerer Str. 2, 67117 Limburgerhof (Germany)

Dr. N. Struch
Current address: Arlanxeo (Deutschland) GmbH
Alte Heerstraße 2, 41540 Dormagen (Germany)

Supporting information and the ORCID identification number(s) for the author(s) of this article can be found under: https://doi.org/10.1002/anie.202108792.

with a nuclearity higher than tetranuclear are known in the literature.[10d,18] This might be due to the fact that classic covalent ligand syntheses to achieve the formation of such structures are often challenging, and therefore, limit the possibility to investigate the influence of different ligands on spin-crossover centres. For this reason, the search for systems that show a spin-transition near room temperature stays demanding.

In 2012 Nitschke et al. presented an impressive heterobimetallic cubic cage with the overall formula $[Fe_8(PtL_4)_6]^{28+}$. This cage contained eight iron(II) centres, coordinated by pyridylimine binding sites with iron centers in the diamagnetic low-spin state. The iron cations were bridged by face-capping tetravalent $[PtL_4]$ building blocks. Making use of the subcomponent self-assembly approach, the synthesis of this cage was rather easily achieved, by combining the precursor platinum(II) building block with 2-formyl pyridine as an azine component together with an iron(II) salt.[5b]

In this work, we want to extend the concept previously established by Nitschke, in order to use this approach for the synthesis of switchable spin-crossover cages. It is known from literature that the exchange of azine building blocks in the final subcomponent self-assembly step with suitable azole building blocks gives the chance to reduce ligand field strength. This reduction of ligand field strength can ultimately result in the stabilization of the paramagnetic high-spin state in iron(II) cations and if carefully performed, can also allow for spin crossover processes.[10d,e,16,17a,b,18,19]

Here, we present three new metallosupramolecular spin-crossover cages, two of which show spin-transition centred near room temperature and one at low temperatures. All three ligands are directly related to each other and can easily be obtained from the same starting material, employing a simple subcomponent self-assembly strategy.[20] We also describe the diamagnetic zinc(II) analogues of all spin-crossover cubes.

Results and Discussion

Synthesis and Characterization

The subcomponent self-assembly approach is a well implemented and powerful tool, not only to simplify ligand (and cage) synthesis, but also to screen a variety of ligand structures in a modular fashion.[20] As this approach already proved useful for the assembly to heterobimetallic structures,[4d–h] we chose to use the robust D_4 symmetric metalloligand **[Pt]** previously introduced by Nitschke[5b] as its tetrafluoroborate salt in order to synthesize the targeted heterobimetallic structures. This precursor can easily be obtained by the assembly of four equivalents 4-(4′-pyridyl)aniline, synthesized according to known literature procedure,[21] with one equivalent of *bis*(acetonitrile) platinum(II) chloride in the presence of two equivalents of silver(I) tetrafluoroborate.[5b] Since the Pt–N bond is remarkably strong,[22] the metalloligand **[Pt]** proved to be stable under ambient conditions for several weeks. Six equivalents of **[Pt]** together with 24 equivalents of aldehyde components 1*H*-4-imidazolecarbaldehyde **1**, *N*-methyl-2-imidazolecarbaldehyde **2** or 4-thiazolecarbaldehyde **3** and 8 equivalents of iron(II) tetrafluoroborate hexahydrate or zinc(II) tetrafluoroborate, respectively, yielded a variety of six tetradecanuclear heterobimetallic cubes $[M_8(Pt\mathbf{L}_4)_6](BF_4)_{28}$ (M = Fe or Zn, **L** = 1-(1*H*-imidazol-4-yl)-*N*-(4-(pyridin-4-yl)phenyl)methanimine, 1-(1-methyl-1*H*-imidazol-2-yl)-*N*-(4-(pyridin-4-yl)phenyl)methanimine) or *N*-(4-(pyridin-4-yl)phenyl)-1-(thiazol-4-yl)methanimine) **[Fe1–3]** and **[Zn1–3]**, respectively (Scheme 1).

The reversible formation of imine bonds in situ and the rather labile character of the iron(II)-nitrogen and zinc(II)-nitrogen bonds ensured rapid cage formation within 12 hours at 65 °C and the isolation of all cubic cages in 87–95 % yield (see SI). The zinc(II) based cages **[Zn1–3]** are fully diamagnetic, and therefore, allowed for comprehensive NMR spectroscopic investigations (see SI). The ^{1}H and ^{13}C NMR spectra of all cages showed one defined set of signals that indicates the presence of *O* symmetric complexes in solution. ^{1}H 2D-DOSY NMR spectra confirmed the formation of discrete structures with solvodynamic radii of 1.58–1.60 nm (Figure 1). The ^{1}H NMR spectra of cubes **[Zn1–3]** also revealed that small amounts of the corresponding aldehydes were present in the samples, even after repeated crystallization and extraction of the complexes. We also found an increasing amount of the free aldehydes and corresponding acids in the ESI MS spectra over several weeks, therefore, the cages **[Zn1–3]** might disintegrate very slowly in solution. The identity of the zinc(II) cubes was further confirmed by electrospray ionization mass spectrometry (ESI MS) and UV/Vis spectroscopy (see SI). The cages containing iron(II) cations could also be identified using ^{1}H NMR[23] and UV/Vis spectroscopy and ESI-MS. **[Fe1–3]** were found to show only one set of signals in the ^{1}H NMR spectra, again indicating *O* symmetric aggregates in solution.

We were able to additionally characterize three of the presented cages in their solid states.[24] **[Fe2]** and **[Fe3]** were crystallized by the slow diffusion of diethyl ether vapour into acetonitrile solutions of the cages, followed by collection of the formed precipitate, extraction with acetonitrile and subsequent slow diffusion of *tert*-butylmethyl ether into the acetonitrile solutions (for details see SI). This procedure gave rise to red blocks of **[Fe2]** and dark red plates of **[Fe3]**. The combination of cryogenic crystal handling and synchrotron radiation[25] allowed for single-crystal structure determination (Figure 2).

In both aggregates the platinum(II) cations occupy the centres of the surfaces of cubic assemblies, coordinated by four 4-pyridyl donors in a square-planar fashion. **[Fe2]** crystallizes in tetragonal space group $P4/n$ with one fourth of the cube in the asymmetric unit and both homochiral enantiomers (all-Λ and all-Δ) were found in the unit cell. The iron(II) cations are coordinated by three *N*-methyl-2-imidazolylimine units in a coordination sphere which is best described as octahedral. The Fe–N bond length at 80 K ranges in between 1.85(3) and 2.20(3) Å. The space diagonal measured as Fe-Fe is 2.88 nm and the Pt-Pt distance of two opposite platinum(II) cations is 1.60 nm. Most likely, the large cavity is filled with disordered solvent molecules and counter anions. **[Fe3]** crystallizes in triclinic space group $P\bar{1}$, with two

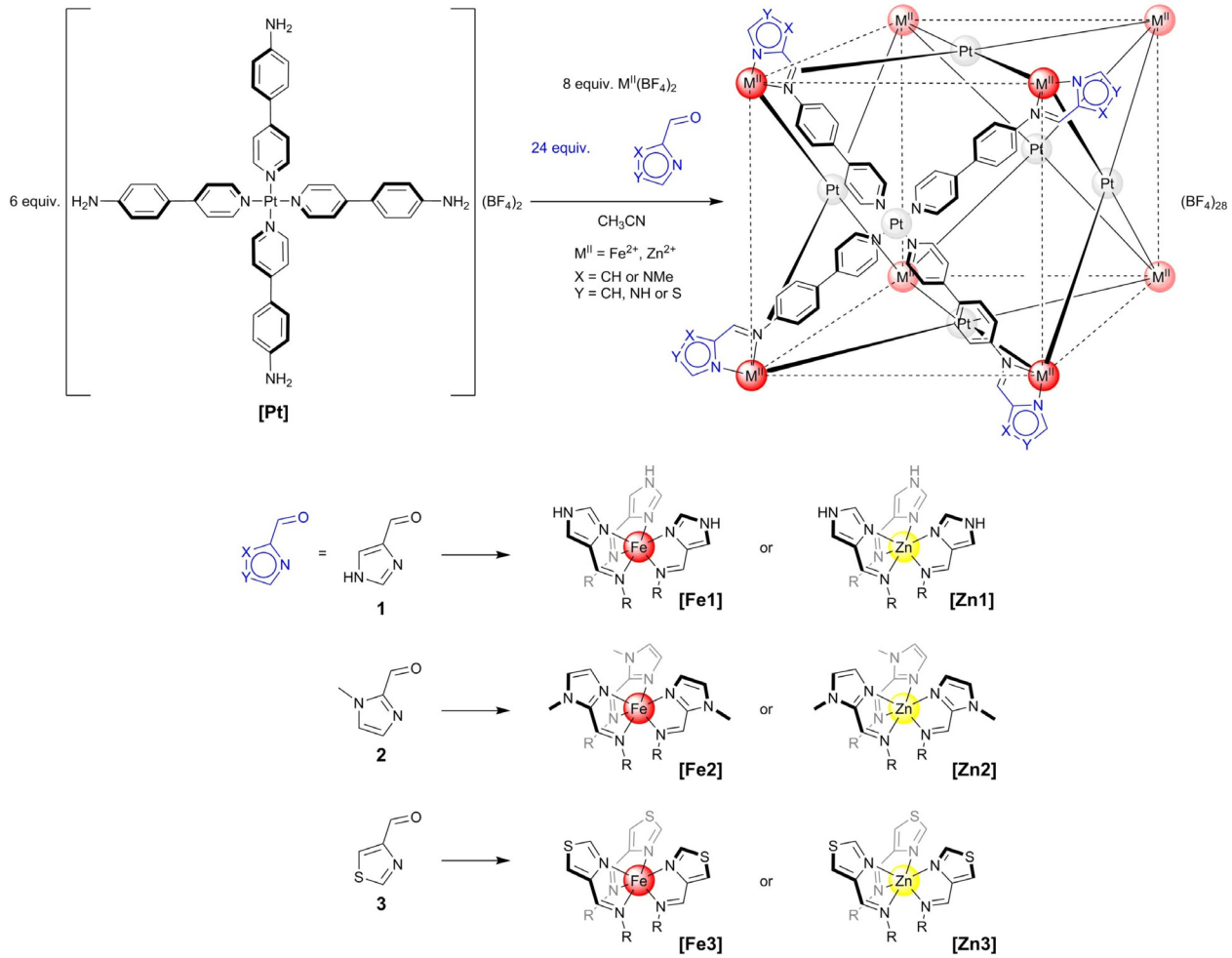

Scheme 1. Synthetic strategy for the preparation of heterobimetallic cubes **[Fe1]**–**[Fe3]** and **[Zn1]**–**[Zn3]** from the same platinum(II) precursor **[Pt]**.

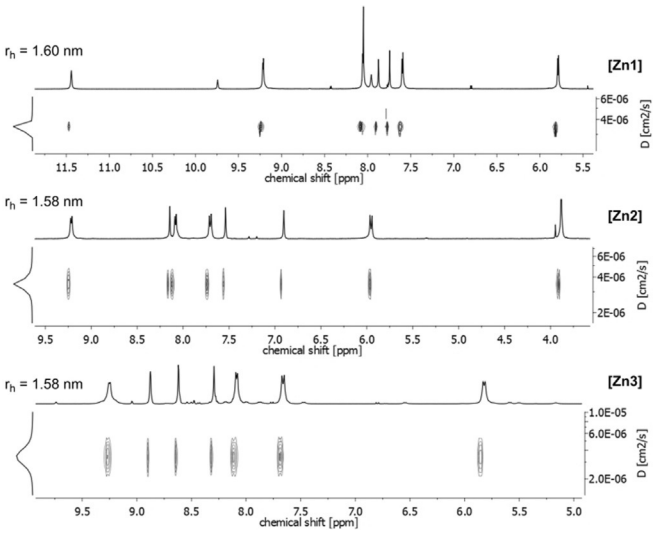

Figure 1. ^{1}H 2D-DOSY spectra (700 MHz, [D$_3$]acetonitrile, 298 K) of **[Zn1]** (r_h = 1.60 nm, top spectrum); **[Zn2]** (r_h = 1.58 nm, spectrum in the middle) and **[Zn3]** (r_h = 1.58 nm, bottom spectrum).

cubes in the asymmetric unit. Analysis was hampered as one of the two cubes is fully disordered and was modelled with two discrete positions. Both homochiral enantiomers are present in the unit cell. Iron(II) cations in **[Fe3]** are coordinated by three 4-thiazolylimine chelating ligands in a similar manner as found with **[Fe2]**. The Fe–N bond length at 80 K ranges between 1.89(2) and 2.06(2) Å. Overall, a very similar dimension of this cage is observed, as already found for **[Fe2]** (Fe-Fe$_{[Fe3]}$ = 2.85 nm; Pt-Pt$_{[Fe3]}$ = 1.65 nm).

One cycle of slow diffusion of *tert*-butylmethyl ether into an acetonitrile solution of **[Zn3]** followed by extraction with acetonitrile yielded transparent yellow plates, which were also suitable to determine its single crystal structure using synchrotron radiation (Figure 2).

[Zn3] crystallizes in triclinic space group $P\bar{1}$ with one full cube in the asymmetric unit and a racemic mixture of the homochiral aggregates. As already found for **[Fe2]** and **[Fe3]** the platinum(II) cations occupy the C_4 symmetry axis of an overall (approximately) O symmetric cubic cage, while zinc-(II) cations build up the C_3 symmetric corners. Each zinc cation is coordinated by three 4-thiazolylimine donors with Zn-N distances ranging between 2.12(3)–2.26(2) Å. Again similar dimensions were found for the space-diagonal Zn-Zn-distances and the distance between two opposite Pt centres (Zn-Zn$_{[Zn3]}$ = 2.88 nm; Pt-Pt$_{[Zn3]}$ = 1.66 nm) which are also in

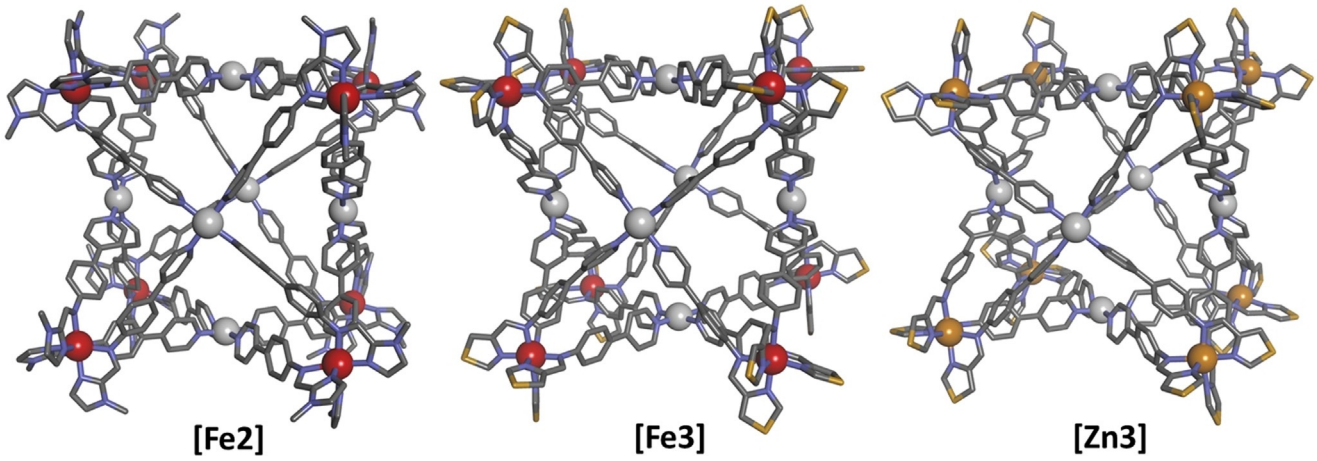

Figure 2. Solid state structures of **[Fe2]** (left), **[Fe3]** (middle) and **[Zn3]** (right) as determined by single crystal X-ray diffraction using synchrotron radiation. Hydrogen atoms, counter anions and solvate molecules are omitted for clarity. Colour code: grey—carbon, red—iron, white—platinum, orange—zinc, blue—nitrogen, yellow—sulphur.

very good agreement to the distances derived from the DOSY NMR experiments.

Magnetic properties of cages [Fe1], [Fe2] and [Fe3]

NMR spectroscopic investigations of the iron(II) containing heterobimetallic cages **[Fe1–3]** showed ^{1}H NMR signals that could not be assigned to purely diamagnetic compounds. While **[Fe1]** showed broadened signals in a range from −9 to +156 ppm which is expected for paramagnetic high-spin iron(II) complexes,[26] cages **[Fe2]** and **[Fe3]** showed signals that suggest the presence of both, high- and low-spin state iron(II) ions at room temperature. The ^{1}H NMR signals of **[Fe2]** were significantly downfield shifted, with chemical shifts up to 88 ppm, whereas the signals of **[Fe3]** showed a less pronounced downfield shift of up to only 45 ppm at room temperature. The observed chemical shifts indicate that the fraction of iron(II) cations in the high-spin state at room temperature follows the order **[Fe1]** > **[Fe2]** > **[Fe3]**, in accordance with the observed downfield shifts. To further investigate the magnetic properties of these cages in acetonitrile solutions, in particular their spin-crossover properties, we performed temperature-dependent Evans' experiments[27] and also used the ideal solution model[28,29,10d,17a] to evaluate our results (Figure 3, SI).[30]

The 4-imidazolylimine cage **[Fe1]** was found to be purely paramagnetic at room temperature,[31] showing a molar magnetic susceptibility multiplied with temperature of $\chi_M T_{298\,K} = 24.9\ cm^3\,K\,mol^{-1}$ (ideal solution model) and $\chi_M T_{298\,K} = 24.9 \pm 1.2\ cm^3\,K\,mol^{-1}$ (Evans' method),[32] respectively. The high-spin state was found to be stable down to a temperature of approximately 245 K. By lowering the temperature even further, we observed the beginning of a spin-crossover process and at 233 K we observed magnetic susceptibilities of $\chi_M T_{233\,K} = 20.8\ cm^3\,K\,mol^{-1}$ (ideal solution model) and $\chi_M T_{233\,K} = 20.8 \pm 0.9\ cm^3\,K\,mol^{-1}$ (Evans' method), which translates to roughly 85 % iron(II) centres still in the paramagnetic high-spin state. Due to the limitation set by the freezing point of acetonitrile we could not follow the spin-crossover to lower temperatures, however, non-linear regression based on the ideal solution model (SI) predicts that the spin transition of **[Fe1]** should be centred at $T_{1/2} = 215$ K (Figure 3 a).

The ^{1}H NMR spectrum of the *N*-methyl-2-imidazolylimine cage **[Fe2]** at room temperature already indicated the presence of both, iron(II) centres in the high- as well as in the low-spin state. This observation was confirmed by our experiments, which revealed a magnetic susceptibility at room temperature of $\chi_M T_{298\,K} = 15.3\ cm^3\,K\,mol^{-1}$ (ideal solution model) and $\chi_M T_{298\,K} = 15.1 \pm 1.2\ cm^3\,K\,mol^{-1}$ (Evans' method). This value corresponds to 63 % of the iron(II) centres in their paramagnetic high-spin state. In accordance to that finding the spin transition temperature of this cage is slightly below room temperature at $T_{1/2} = 281$ K (Figure 3 b).

Within the temperature-limitations set by the solvent we could not observe a purely paramagnetic or diamagnetic situation of the complex. At 343 K the magnetic susceptibility is $\chi_M T_{343\,K} = 20.5\ cm^3\,K\,mol^{-1}$ (ideal solution model) and $\chi_M T_{343\,K} = 20.3 \pm 1.3\ cm^3\,K\,mol^{-1}$ (Evans' method) (≈ 84 % high-spin iron(II) centres) and at 233 K it is $\chi_M T_{233\,K} = 0.8\ cm^3\,K\,mol^{-1}$ (ideal solution model). However, at 233 K the situation is very close to fully diamagnetic, and therefore, employing the Evans' method becomes prone to errors in measurements (discussion in SI).

The 4-thiazolylimine cage **[Fe3]** showed the less pronounced downfield shift of ^{1}H-NMR signals at room temperature, indicating the highest fraction of low-spin iron(II) centres at this temperature within the investigated complexes. Indeed, the magnetic susceptibility at room temperature turned out to be only $\chi_M T_{298\,K} = 5.6\ cm^3\,K\,mol^{-1}$ (ideal solution model) and $\chi_M T_{298\,K} = 5.9 \pm 1.1\ cm^3\,K\,mol^{-1}$ (Evans' method), which translates to 77 % iron(II) centres in the diamagnetic low-spin state. At 233 K even no magnetic susceptibility could be measured using the Evans' method, whereas the ideal solution model yielded the very small value $\chi_M T_{233\,K} = 0.1\ cm^3\,K\,mol^{-1}$. At high temperatures, on the other hand, the fraction of high-spin centres becomes significantly larger

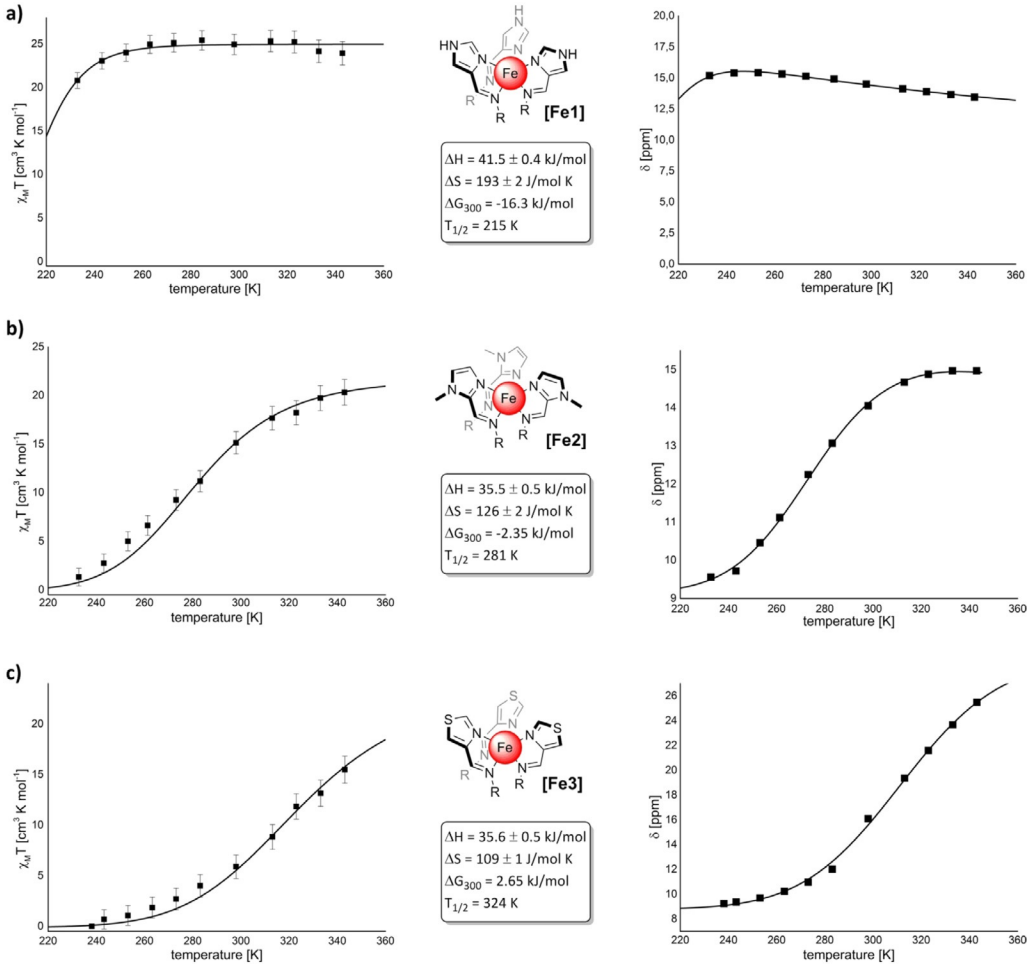

Figure 3. Calculated molar magnetic susceptibilities multiplied with temperature $\chi_M T$ based on the ideal solution model (left column, squares are values obtained from the Evans method with calculated error bars and the lines are the non-linear regressions following the ideal solution model.) for a) **[Fe1]**, b) **[Fe2]** and c) **[Fe3]** and the corresponding temperature-dependent ^{1}H NMR shifts of selected protons in [D$_3$]acetonitrile (black squares, lines correspond to the non-linear regressions following the ideal solution model in the right column). The boxes summarize thermodynamic data based on the ideal solution model. Please note: For **[Fe3]** we chose a ^{1}H-NMR signal with a more pronounced downfield shift, compared to **[Fe1]** and **[Fe2]**. This was done for sake of precision, by choosing signals that were easy to follow and could be located precisely. However, the overall NMR spectra show that the downfield shift is less pronounced for **[Fe3]**.

and at 343 K we determined the magnetic susceptibility as $\chi_M T_{343\,K} = 15.9\ cm^3\,K\,mol^{-1}$ (ideal solution model) and $\chi_M T_{343\,K} = 15.5 \pm 1.3\ cm^3\,K\,mol^{-1}$ (Evans' method), showing that **[Fe3]** shows the highest spin transition temperature of the investigated cages. The spin-crossover of this complex is located at $T_{1/2} = 324$ K, slightly above room temperature (Figure 3c).

The ideal solution model does not only yield magnetic susceptibilities, but also can be used to obtain thermodynamic data from temperature-dependent ^{1}H NMR experiments (Figure 3, details SI). As the spin-crossover phenomenon is a mainly entropically driven process[9d] the calculated transition entropies ΔS increase with decreasing transition temperatures. In other words, the transition entropy of the system is high, when the stabilization of the paramagnetic high-spin state is high. Accordingly, we observed ΔS(**[Fe1]**) > ΔS(**[Fe2]**) > ΔS(**[Fe3]**). Furthermore, the calculated transition enthalpies ΔH and transition entropies ΔS suggest that ΔG_{300} for **[Fe1]** and **[Fe2]** is negative, meaning that the high-spin state is actually the favoured state at 300 K, while ΔG_{300} for **[Fe3]** is positive, and therefore, indicates that the high-spin state is less favoured than the low-spin state for this cage at 300 K. These findings are in accordance with the determined transition temperatures, which are below 300 K for **[Fe1]** and **[Fe2]**, but above 300 K for **[Fe3]**. In addition, this finding is in line with results obtained from other studies, investigating the influence of different azole building blocks on the spin-crossover behaviour of iron(II) cations, where thiazoles are regularly found to yield the strongest ligand field amongst azoles and consequently result in the highest spin transition temperatures.[10e,16b,c,19]

Conclusion

In this work we presented the modular synthesis of six heterobimetallic cubic cages, all starting from the same D_4 symmetric platinum(II) metalloligand **[Pt]**. The final chelat-

ing units were readily assembled through subcomponent self-assembly, which allowed for the easy synthesis of three directly related ligands by using 1*H*-4-imidazolecarbaldehyde **1**, *N*-methyl-2-imidazolecarbaldehyde **2** or 4-thiazolecarbaldehyde **3** as subcomponents. The use of zinc(II) salts yielded the diamagnetic cages **[Zn1–3]**, which allowed for comprehensive NMR spectroscopic investigations of these complexes. Instead, the use of iron(II) salts gave rise to cages **[Fe1–3]**, which showed spin-crossover properties in solution. We also could characterize three of these large tetradecanuclear cages in their solid states.

We further investigated the magnetic behaviour of the iron(II) containing spin-crossover cages in acetonitrile solutions, employing both, the Evans' method and the ideal solution model. While **[Fe1]** showed a spin transition temperature at a low temperature ($T_{1/2}$(**[Fe1]**) = 215 K), the cages **[Fe2]** and **[Fe3]** showed transition temperatures around room temperature ($T_{1/2}$(**[Fe2]**) = 281 K; $T_{1/2}$(**[Fe3]**) = 324 K), which is much more beneficial for potential applications centred around room temperature. Metallosupramolecular chemistry, especially the subcomponent self-assembly approach, proved to be an easy-to-use tool to tune the complex properties, by simply exchanging ligand building blocks. Anyway, the cages **[Fe1–3]** expand the number of known octanuclear iron(II) spin-crossover cages, which are rarely found in the literature so far.[10d,13a] These cages might also show the huge potential of iron(II) cages with high nuclearities as molecular switches that can be easily obtained by also including platinum(II) as a second type of metal cation, ensuring the rapid assembly from small and simple building blocks. The large cavities of the presented assemblies might also allow for guest uptake, which may be an additional chance to manipulate the spin-crossover process and will be explored in future works.

Acknowledgements

M.H. thanks the Jürgen-Manchot foundation for a doctoral scholarship. N.S. is thankful to the Evonic Foundation for a doctoral grant. Financial support from the DFG, SFB 813 "Chemistry at Spin Centers" is gratefully acknowledged. S.H. thanks the JSPS Program for Advancing Strategic International Networks to Accelerate the Circulation on Talented Researchers. G.H.C., J.T., and J.J.H. thank the European Research Council (ERC Consolidator grant 683083, RAMSES) for supporting this study. Diffraction data of **[Fe2]**, **[Fe3]**, and **[Zn3]** were collected at PETRA III at DESY, a member of the Helmholtz Association (HGF). The authors thank Eva Crosas and Olga Lorbeer for assistance in using synchrotron beam line P11 (I-20180412). Open access funding enabled and organized by Projekt DEAL.

Conflict of Interest

The authors declare no conflict of interest.

Keywords: heterobimetallic cages · iron · metallosupramolecular chemistry · spin crossover · subcomponent self-assembly

[1] *For some reviews see*: a) R. Chakrabarty, P. S. Mukherjee, P. J. Stang, *Chem. Rev.* **2011**, *111*, 6810 – 6918; b) M. M. J. Smulders, I. A. Riddell, C. Browne, J. R. Nitschke, *Chem. Soc. Rev.* **2013**, *42*, 1728 – 1754; c) K. Harris, D. Fujita, M. Fujita, *Chem. Commun.* **2013**, *49*, 6703 – 6712; d) L. Chen, Q. Chen, M. Wu, F. Jiang, M. Hong, *Acc. Chem. Res.* **2015**, *48*, 201 – 210; e) C. J. Brown, F. D. Toste, R. G. Bergman, K. N. Raymond, *Chem. Rev.* **2015**, *115*, 3012 – 3035; f) T. R. Cook, P. J. Stang, *Chem. Rev.* **2015**, *115*, 7001 – 7045.

[2] a) M. Fujita, M. Tominaga, A. Hori, B. Therrien, *Acc. Chem. Res.* **2005**, *38*, 369 – 378; b) T. R. Cook, Y.-R. Zheng, P. J. Stang, *Chem. Rev.* **2013**, *113*, 734 – 777; c) L.-J. Chen, H.-B. Yang, M. Shinoya, *Chem. Soc. Rev.* **2017**, *46*, 2555 – 2576; d) S. Mukherjee, P. S. Mukherjee, *Chem. Commun.* **2014**, *50*, 2239 – 2248; e) M. Han, D. M. Engelhard, G. H. Clever, *Chem. Soc. Rev.* **2014**, *43*, 1848 – 1860.

[3] a) R. Zhu, J. Lübben, B. Dittrich, G. H. Clever, *Angew. Chem. Int. Ed.* **2015**, *54*, 2796 – 2800; *Angew. Chem.* **2015**, *127*, 2838 – 2842; b) T. Zhang, L.-P. Zhou, X.-Q. Guo, L.-X. Cai, Q.-F. Sun, *Nat. Commun.* **2017**, *8*, 15898; c) M. Käseborn, J. J. Holstein, G. H. Clever, A. Lützen, *Angew. Chem. Int. Ed.* **2018**, *57*, 12171 – 12175; *Angew. Chem.* **2018**, *130*, 12349 – 12353; d) J. Anhäuser, R. Puttreddy, L. Glanz, A. Schneider, M. Engeser, K. Rissanen, A. Lützen, *Chem. Eur. J.* **2019**, *25*, 12294 – 12297.

[4] a) F. Reichel, J. K. Clegg, K. Gloe, J. J. Weigand, J. K. Reynolds, C.-G. Li, J. R. Aldrich-Wright, C. J. Kepert, L. F. Lindoy, H.-C. Yao, F. Li, *Inorg. Chem.* **2014**, *53*, 688 – 690; b) S. M. Jansze, M. D. Wise, A. V. Vologzhanina, R. Scopelliti, K. Severin, *Chem. Sci.* **2017**, *8*, 1901 – 1908; c) I. Sinha, P. S. Mukherjee, *Inorg. Chem.* **2018**, *57*, 4205 – 4221; d) R. Saha, D. Samanta, A. J. Bhattacharyya, P. S. Mukherjee, *Chem. Eur. J.* **2017**, *23*, 8980 – 8986; e) M. Hardy, N. Struch, F. Topić, G. Schnakenburg, K. Rissanen, A. Lützen, *Inorg. Chem.* **2018**, *57*, 3507 – 3515; f) W. J. Ramsay, F. T. Szczypiński, H. Weissman, T. K. Ronson, M. M. J. Smulders, B. Rybtchinski, J. R. Nitschke, *Angew. Chem. Int. Ed.* **2015**, *54*, 5636 – 5640; *Angew. Chem.* **2015**, *127*, 5728 – 5732; g) Y. Yang, Y. Wu, J.-H. Jia, X.-Y. Zheng, Q. Zhang, K.-C. Xiong, Z.-M. Zhang, Q.-M. Wang, *Cryst. Growth Des.* **2018**, *18*, 4555 – 4561; h) W.-K. Han, H.-X. Zhang, Y. Wang, W. Liu, X. Yan, T. Li, Z.-G. Gu, *Chem. Commun.* **2018**, *54*, 12646 – 12649.

[5] a) W. J. Ramsay, J. R. Nitschke, *J. Am. Chem. Soc.* **2014**, *136*, 7038; b) M. M. J. Smulders, A. Jiménez, J. R. Nitschke, *Angew. Chem. Int. Ed.* **2012**, *51*, 6681 – 6685; *Angew. Chem.* **2012**, *124*, 6785 – 6789; c) F. E. Hahn, M. Offermann, C. Schulze Isfort, T. Pape, R. Fröhlich, *Angew. Chem. Int. Ed.* **2008**, *47*, 6794 – 6797; *Angew. Chem.* **2008**, *120*, 6899 – 6902; d) H.-B. Wu, Q.-M. Wang, *Angew. Chem. Int. Ed.* **2009**, *48*, 7343 – 7345; *Angew. Chem.* **2009**, *121*, 7479 – 7481; e) C. Colomban, V. Martin-Diaconescu, T. Parella, S. Goeb, C. Garciá-Simón, J. Lloret-Fillol, M. Costas, X. Ribas, *Inorg. Chem.* **2018**, *57*, 3529 – 3539; f) S. Hiraoka, Y. Sakata, M. Shionoya, *J. Am. Chem. Soc.* **2008**, *130*, 10058 – 10059; g) H. Li, Z.-J. Yao, D. Liu, G.-X. Jin, *Coord. Chem. Rev.* **2015**, *293 – 294*, 139 – 157.

[6] A. B. Wragg, A. J. Metherell, W. Cullen, M. D. Ward, *Dalton Trans.* **2015**, *44*, 17939 – 17949.

[7] a) M. Wang, V. Vajpayee, S. Shanmugaraju, Y.-R. Zheng, Z. Zhao, H. Kim, P. S. Mukherjee, K.-W. Chi, P. J. Stang, *Inorg. Chem.* **2011**, *50*, 1506 – 1512; b) K. Li, L.-Y. Zhang, C. Yan, S.-C. Wie, M. Pan, L. Zhang, C.-Y. Su, *J. Am. Chem. Soc.* **2014**, *136*, 4456 – 4459.

[8] a) C. Aronica, G. Pilet, G. Chastanet, W. Wernsdorfer, J.-F. Jacquot, D. Luneau, *Angew. Chem. Int. Ed.* **2006**, *45*, 4659 – 4662; *Angew. Chem.* **2006**, *118*, 4775 – 4778; b) S. Sanz, H. M. O'Con-

nor, E. M. Pineda, K. S. Pedersen, G. S. Nichol, O. Mønsted, H. Weihe, S. Piligkos, E. J. L. McInnes, P. J. Lusby, E. K. Brechin, *Angew. Chem. Int. Ed.* **2015**, *54*, 6761 – 6764; *Angew. Chem.* **2015**, *127*, 6865 – 6868; c) L. Li, Y. Zhang, M. Avdeev, L. F. Lindoy, D. G. Harman, R. Zheng, Z. Cheng, J. R. Aldrich-Wright, F. Li, *Dalton Trans.* **2016**, *45*, 9407 – 9411; d) J. Guo, Y.-W. Xu, K. Li, L.-M. Xiao, S. Chen, K. Wu, X.-D. Chen, Y.-Z. Fan, J.-M. Liu, C.-Y. Su, *Angew. Chem. Int. Ed.* **2017**, *56*, 3852 – 3856; *Angew. Chem.* **2017**, *129*, 3910 – 3914.

[9] a) L. Cambi, L. Szegö, *Ber. Dtsch. Chem. Ges. B* **1931**, *64*, 2591 – 2598; b) K. Madeja, E. König, *J. Inorg. Nucl. Chem.* **1963**, *25*, 377 – 385; c) *Spin-Cossover Materials* (Ed.: M. A. Halcrow), Wiley, Chichester, **2013**; d) P. Gütlich, A. Hauser, H. Spiering, *Angew. Chem. Int. Ed. Engl.* **1994**, *33*, 2024 – 2054; *Angew. Chem.* **1994**, *106*, 2109 – 2141.

[10] a) D.-H. Ren, D. Qiu, C.-Y. Pang, Z. Li, Z.-G. Gu, *Chem. Commun.* **2015**, *51*, 788 – 791; b) D. Shao, L. Shi, L. Yin, B.-L. Wang, Z.-X. Wang, Y.-Q. Zhang, X.-Y. Wang, *Chem. Sci.* **2018**, *9*, 7986 – 7991; c) C. Lochenie, K. Schötz, F. Panzer, H. Kurz, B. Maier, F. Puchtler, S. Agarwal, A. Köhler, B. Weber, *J. Am. Chem. Soc.* **2018**, *140*, 700 – 709; d) N. Struch, C. Bannwarth, T. K. Ronson, Y. Lorenz, B. Mienert, N. Wagner, M. Engeser, E. Bill, R. Puttreddy, K. Rissanen, J. Beck, S. Grimme, J. R. Nitschke, A. Lützen, *Angew. Chem. Int. Ed.* **2017**, *56*, 4930 – 4935; *Angew. Chem.* **2017**, *129*, 5012 – 5017; e) N. Struch, N. Wagner, G. Schnakenburg, R. Weisbarth, S. Klos, J. Beck, A. Lützen, *Dalton Trans.* **2016**, *45*, 14023 – 14029.

[11] a) M. Seredyuk, A. B. Gaspar, V. Ksenofontov, M. Verdaguer, F. Villain, P. Gütlich, *Inorg. Chem.* **2009**, *48*, 6130 – 6141; b) I. C. Berdiell, T. Hochdörffer, C. Desplanches, R. Kulmaczewski, N. Shahid, J. A. Wolny, S. L. Warriner, O. Cespedes, V. Schünemann, G. Chastanet, M. A. Halcrow, *J. Am. Chem. Soc.* **2019**, *141*, 18759 – 18770.

[12] a) A. Bhattacharjee, M. Roy, V. Ksenofontov, J. A. Kitchen, S. Brooker, P. Gütlich, *Eur. J. Inorg. Chem.* **2013**, 843 – 849; b) A. Bhattacharjee, V. Ksenofontov, H. A. Goodwin, P. Gütlich, *J. Phys. Condens. Matter* **2009**, *21*, 026011.

[13] a) R. W. Hogue, S. Singh, S. Brooker, *Chem. Soc. Rev.* **2018**, *47*, 7303 – 7338; b) S. Brooker, *Chem. Soc. Rev.* **2015**, *44*, 2880 – 2892; c) P. Gütlich, H. A. Goodwin, *Top. Curr. Chem.* **2004**, *233*, 1 – 47; d) K. S. Kumar, M. Ruben, *Coord. Chem. Rev.* **2017**, *346*, 176 – 205.

[14] a) I.-R. Jeon, J. G. Park, C. R. Haney, T. D. Harris, *Chem. Sci.* **2014**, *5*, 2461 – 2465; b) R. G. Miller, S. Brooker, *Chem. Sci.* **2016**, *7*, 2501 – 2505; c) J. Krober, E. Codjovi, O. Kahn, F. Groliere, C. Jay, *J. Am. Chem. Soc.* **1993**, *115*, 9810 – 9811; d) P. Gütlich, Y. Garcia, H. A. Goodwin, *Chem. Soc. Rev.* **2000**, *29*, 419 – 427; e) A. B. Gaspar, V. Ksenofontov, M. Seredyuk, P. Gütlich, *Coord. Chem. Rev.* **2005**, *249*, 2661 – 2676; f) A. Bousseksou, G. Molnár, J. A. Real, K. Tanaka, *Coord. Chem. Rev.* **2007**, *251*, 1822 – 1833; g) K. S. Murray, *Eur. J. Inorg. Chem.* **2008**, 3101 – 3121; h) A. J. McConnell, *Supramol. Chem.* **2018**, *30*, 858 – 868.

[15] a) E. Breuning, M. Ruben, J.-M. Lehn, F. Renz, Y. Garcia, V. Ksenofontov, P. Gütlich, E. Wegelius, K. Rissanen, *Angew. Chem. Int. Ed.* **2000**, *39*, 2504 – 2507; *Angew. Chem.* **2000**, *112*, 2563 – 2566; b) M. Ruben, E. Breuning, J.-M. Lehn, V. Ksenofontov, F. Renz, P. Gütlich, G. B. M. Vaughan, *Chem. Eur. J.* **2003**, *9*, 4422 – 4431 (including erratum *Chem. Eur. J.* **2003**, *9*, 5176); c) L. H. Uppadine, J.-P. Gisselbrecht, N. Kyritsakas, K. Nättinen, K. Rissanen, J.-M. Lehn, *Chem. Eur. J.* **2005**, *11*, 2549 – 2565; d) M. Nihei, M. Ui, M. Yokota, L. Han, A. Maeda, H. Kishida, H. Okamoto, H. Oshio, *Angew. Chem. Int. Ed.* **2005**, *44*, 6484 – 6487; *Angew. Chem.* **2005**, *117*, 6642 – 6645; e) B. Schneider, S. Demeshko, S. Dechert, F. Meyer, *Angew. Chem. Int. Ed.* **2010**, *49*, 9274 – 9277; *Angew. Chem.* **2010**, *122*, 9461 – 9464; f) Y.-T. Wang, S.-T. Li, S.-Q. Wu, A.-L. Cui, D.-Z. Shen, H.-Z. Kou, *J. Am. Chem. Soc.* **2013**, *135*, 5942 – 5945; g) M. U. Anwar, L. N. Dawe, S. R. Parsons, S. S. Tandon, L. K. Thompson, S. K. Dey, V. Mereacre, W. M. Reiff, S. D. Bunge, *Inorg. Chem.* **2014**, *53*, 4655 – 4668; h) O. Hietsoi, P. W. Dunk, H. D. Stout, A. Arroyave, K. Kovnir, R. E. Irons, N. Kassenova, R. Erkasov, C. Achim, M. Shatruk, *Inorg. Chem.* **2014**, *53*, 13070 – 13077; i) M. Steinert, B. Schneider, S. Dechert, S. Demeshko, F. Meyer, *Angew. Chem. Int. Ed.* **2014**, *53*, 6135 – 6139; *Angew. Chem.* **2014**, *126*, 6249 – 6253; j) T. Matsumoto, G. N. Newton, T. Shiga, S. Hayami, Y. Matsui, H. Okamoto, R. Kumai, Y. Murakami, H. Oshio, *Nat. Commun.* **2014**, *5*, 3865; k) M. Steinert, B. Schneider, S. Dechert, S. Demenshko, F. Meyer, *Inorg. Chem.* **2016**, *55*, 2363 – 2373; l) B. Schäfer, J.-F. Greisch, I. Faus, T. Bodenstein, I. Šalitroš, O. Fuhr, K. Fink, V. Schünemann, M. M. Kappes, M. Ruben, *Angew. Chem. Int. Ed.* **2016**, *55*, 10881 – 10885; *Angew. Chem.* **2016**, *128*, 11040 – 11044; m) S. Dhers, A. Mondal, D. Aguilà, J. Ramírez, S. Vela, P. Dechambenoit, M. Rouzières, J. R. Nitschke, R. Clerác, J.-M. Lehn, *J. Am. Chem. Soc.* **2018**, *140*, 8218 – 8227; n) T. Shiga, Y. Sato, M. Tachibana, H. Sato, T. Matsumoto, H. Sagayama, R. Kumai, Y. Murakami, G. N. Newton, H. Oshio, *Inorg. Chem.* **2018**, *57*, 14013 – 14017; o) I. Šalitroš, R. Herchel, O. Fuhr, R. González-Preto, M. Ruben, *Inorg. Chem.* **2019**, *58*, 4310 – 4319; p) J. W. Shin, A. R. Jeong, J. H. Jeong, H. Zenno, S. Hayami, S. Kil, *RSC Adv.* **2020**, *10*, 5040 – 5049; q) Y. Uezu, R. Tsunashima, C. Tanaka, M. Fujibayashi, J. Masaru, S. Nishihara, K. Inoue, *Bull. Chem. Soc. Jpn.* **2020**, *93*, 1583 – 1587.

[16] a) D. Pelleteret, R. Clérac, C. Mathonière, E. Harte, W. Schmitt, P. E. Kruger, *Chem. Commun.* **2009**, 221 – 223; b) L. Li, A. R. Craze, R. Akiyoshi, A. Tsukiashi, S. Hayami, O. Mustonen, M. M. Bhadbhade, S. Bhattacharyya, C. E. Marjo, Y. Wang, L. F. Lindoy, J. R. Aldrich-Wright, F. Li, *Dalton Trans.* **2018**, *47*, 2543 – 2548; c) S. Singh, S. Brooker, *Chem. Sci.* **2021**, https://doi.org/10.1039/d1sc01458g.

[17] a) A. Ferguson, M. A. Squire, D. Siretanu, D. Mitcov, C. Mathonière, R. Clérac, P. E. Kruger, *Chem. Commun.* **2013**, *49*, 1597 – 1599; b) F. L. Zhang, J.-Q. Chen, L.-F. Qin, L. Tian, Z. Li, X. Ren, Z.-G. Gu, *Chem. Commun.* **2016**, *52*, 4796 – 4799.

[18] a) M. B. Duriska, S. M. Neville, B. Moubaraki, J. D. Cashion, G. J. Halder, K. W. Chapman, C. Balde, J.-F. Létard, K. S. Murray, C. J. Kepert, S. R. Batten, *Angew. Chem. Int. Ed.* **2009**, *48*, 2549 – 2552; *Angew. Chem.* **2009**, *121*, 2587 – 2590; b) Z. Yan, W. Liu, Y.-Y. Peng, Y.-C. Chen, Q.-W. Li, Z.-P. Ni, M.-L. Tong, *Inorg. Chem.* **2016**, *55*, 4891 – 4896.

[19] a) S. Singh, S. Brooker, *Inorg. Chem.* **2020**, *59*, 1265 – 1273; b) C. F. Herold, S. I. Shylin, E. Rentschler, *Inorg. Chem.* **2016**, *55*, 6414 – 6419.

[20] a) A. M. Castilla, W. J. Ramsay, J. R. Nitschke, *Acc. Chem. Res.* **2014**, *47*, 2063 – 2073; b) J. R. Nitschke, *Acc. Chem. Res.* **2007**, *40*, 103 – 112.

[21] R. Li, M. P. Martin, Y. Liu, B. Wang, R. A. Patel, J.-Y. Zhu, N. Sun, R. Pireddu, N. J. Lawrence, J. Li, E. B. Haura, S.-S. Sung, W. C. Guida, E. Schonbrunn, S. M. Sebti, *J. Med. Chem.* **2012**, *55*, 2474 – 2478.

[22] D. Fujita, A. Takahashi, S. Sato, M. Fujita, *J. Am. Chem. Soc.* **2011**, *133*, 13317 – 13319.

[23] Please note, that very recently a first study was reported on the extension of the paramagnetic NMR spectroscopy toolbox for the characterization of paramagnetic and spin-crossover metallosupramolecular aggregates, see M. Lehr, T. Paschelke, E. Trumpf, A.-M. Vogt, C. Näther, F. D. Sönnichsen, A. J. McConnell, *Angew. Chem. Int. Ed.* **2020**, *59*, 19344 – 19351; *Angew. Chem.* **2020**, *132*, 19508 – 19516.

[24] Crystallographic data for cubic assemblies **[Fe2]**, **[Fe3]** and **[Zn3]** can be obtained free of charge from the joint Cambridge Crystallographic Data Centre and Fachinformationszentrum Karlsruhe Access Structures service, deposition numbers 2067864, 2067865, 2067866.

[25] A. Burkhardt, T. Pakendorf, B. Reime, J. Meyer, P. Fischer, N. Stübe, S. Panneerselvam, O. Lorbeer, K. Stachnik, M. Warmer, P. Rödig, D. Göries, A. Meents, *Eur. Phys. J. Plus* **2016**, *131*, 56.
[26] W. C. Isley III, S. Zarra, R. K. Carlson, R. A. Bilbesi, T. K. Ronson, J. R. Nitschke, L. Gagliardi, C. J. Cramer, *Phys. Chem. Chem. Phys.* **2014**, *16*, 10620 – 10628.
[27] D. F. Evans, *J. Chem. Soc.* **1959**, 2003 – 2005.
[28] W. Klaeui, W. Eberspach, P. Gütlich, *Inorg. Chem.* **1987**, *26*, 3977 – 3982.
[29] *For some examples on the application of the ideal solution model see*: a) S. G. Telfer, B. Bocquet, A. F. Williams, *Inorg. Chem.* **2001**, *40*, 4818 – 4820; b) J. Travieso-Puente, J. O. P. Broekman, M.-C. Chang, S. Demeshko, F. Meyer, E. Otten, *J. Am. Chem. Soc.* **2016**, *138*, 5503 – 5506.
[30] Please note that we also tried to investigate the magnetic behaviour of the complexes **[Fe1–3]** in the solid state using a vibrating sample magnetometer, but due to the very rapid solvent loss of the used crystals, the measurements did not yield reasonable results (see SI). A differential scanning calorimetry (DSC) measurement with **[Fe3]** also did not lead to insights into the processes upon temperature-changes because the transition is too gradual to cause large enough effects detectable with this technique (SI).
[31] Per uncoupled iron(II) cation in the paramagnetic high-spin state a value of $\chi_M T = 3.001\ cm^3 K mol^{-1}$ is expected, see ref. [15a].
[32] The calculation of uncertainties is discussed in the SI.

Manuscript received: July 2, 2021
Revised manuscript received: August 4, 2021
Accepted manuscript online: August 12, 2021
Version of record online: September 6, 2021

